QUIC-PLUME Theory Guide

Last updated: 1-26-04

Michael D. Williams, Michael J. Brown, Balwinder Singh, and David Boswell
Los Alamos National Laboratory
Infrastructure and Energy Analysis, Group D-4, MS F604
Los Alamos, NM USA 87545

Introduction

The Quick Urban & Industrial Complex (QUIC) Dispersion Modeling System is intended for applications where dispersion of airborne contaminants released near buildings must be computed quickly. QUIC is composed of a wind model, QUIC-URB, a dispersion model, QUIC-PLUME, and a graphical user interface, QUIC-GUI. This document describes the QUIC-PLUME model equations, the special considerations needed for urban applications, and assumptions made in the turbulence parameterizations. Companion documents describe the QUIC-URB model (Pardyjak, 2004), how to run QUIC-PLUME in standalone mode (Williams, 2004), and how to use the QUIC-GUI (Boswell and Brown, 2004).

Model Overview

Buildings produce complex flows that pose difficult challenges to dispersion modelers. The QUIC-URB model uses an empirical-diagnostic approach to compute a mass consistent 3D wind field around buildings (e.g., Pardyjak and Brown, 2001). The QUIC-PLUME model is a Lagrangian dispersion model that uses the mean wind fields from QUIC-URB and turbulent winds computed internally using the Langevin random walk equations. Gradients in the wind fields are used to estimate the turbulence parameters.

The QUIC-PLUME code does not use the traditional three term random-walk equation that has been used successfully for boundary layer flow problems. Due to the horizontal inhomogeneity of the flow around buildings, the code uses more terms and a unique coordinate rotation approach in order to account for lateral and vertical mean motions and horizontal gradients in turbulence parameters. The code has undergone a series of changes from its initial formulation, including: (1) calculating dissipation with a revised method, (2) computing turbulence parameters from local gradients, 3) adding two additional drift terms, and (4) developing a new non-local mixing formulation. These last two changes significantly improved model performance and are shown at the end of this document.

Lagrangian particle physics in inhomogeneous turbulence in the surface layer

Lagrangian particle models describe dispersion by simulating the releases of particles and moving them with an instantaneous wind composed of a mean wind plus a turbulent wind. The equations that describe the positions of particles are:

$$x = x_p + U\Delta t + \frac{u_p + u}{2}\Delta t,$$

$$y = y_p + V\Delta t + \frac{v_p + v}{2}\Delta t,$$

and

$$z = z_p + W\Delta t + \frac{w_p + w}{2}\Delta t,$$

where *x, y,* and *z* are the current position coordinates of the particle and the subscript p refers to the previous positions. *U, V,* and *W* are the mean winds while u', v', and w' are the fluctuating components of the instantaneous wind and Δt is the time step. Mean winds are winds averaged over a sufficient length of time (usually 10 minutes to an hour) to remove the effects of random fluctuations.

The fluctuating components of the instantaneous winds are calculated from:

$$u' = u_p' + du,$$

$$v' = v_p' + dv,$$

and,

$$w' = w_p' + dw.$$

Generally, the equations for *du, dv,* and *dw* are quite complicated:

$$du_i = -\frac{Co\varepsilon}{2}\sum_{k=1}^{3} a_{ik}\left(u_k - U_k\right)dt + \sum_{j=1}^{3} U_j \frac{\partial U_i}{\partial x_j}dt +$$

$$\sum_{j=1}^{3}\left[\frac{\partial U_i}{\partial x_j} + \sum_{m=1}^{3}\frac{a_{im}}{2}\sum_{k=1}^{3} U_k \frac{\partial a_{km}}{\partial x_j}\right]\left(u_j - U_j\right)dt +$$

$$\sum_{m=1}^{3}\frac{a_{im}}{2}\sum_{k=1}^{3}\sum_{j=1}^{3}\frac{\partial a_{km}}{\partial x_j}\left(u_j - U_j\right)\left(u_k - U_k\right)dt +$$

$$\frac{1}{2}\sum_{j=1}^{3}\frac{\partial \tau_{ij}}{\partial xj}dt + (Co\varepsilon dt)^{1/2}dW_i(t),$$

but dramatic simplifications can be made if the mean vertical wind W is zero, the mean horizontal winds are uniform and the coordinate system is rotated so that the mean wind is in the x-direction ($V=W=0$). Under these circumstances (Rodean, 1996, pages 43-44), the expressions for du, dv, and dw are:

$$du = \left[\frac{Co\varepsilon}{2}\left[\sigma_{11}(u-U)+\sigma_{13}w\right]+\frac{\partial U}{\partial z}w+\frac{1}{2}\frac{\partial \sigma_{13}}{\partial z}\right]dt+$$
$$\left[\frac{\partial \sigma_{11}}{\partial z}\left[\sigma_{11}(u-U)+\sigma_{13}w\right]+\frac{\partial \sigma_{13}}{\partial z}\left[\sigma_{13}(u-U)+\sigma_{33}w\right]\right]\frac{w}{2}dt+$$
$$(Co\varepsilon dt)^{1/2}dW_1(t),$$

$$dv = \left[\frac{Co\varepsilon}{2}(\sigma_{22}v)+\frac{\partial \sigma_{22}}{\partial z}(\sigma_{22}v)\frac{w}{2}\right]dt+(Co\varepsilon dt)^{1/2}dW_2(t),$$

and,

$$dw = \left[\frac{Co\varepsilon}{2}\left[\sigma_{13}(u-U)+\sigma_{33}w\right]+\frac{1}{2}\frac{\partial \sigma_{33}}{\partial z}\right]dt+$$
$$\left[\frac{\partial \sigma_{13}}{\partial z}\left[\sigma_{11}(u-U)+\sigma_{13}w\right]+\frac{\partial \sigma_{33}}{\partial z}\left[\sigma_{13}(u-U)+\sigma_{33}w\right]\right]\frac{w}{2}dt+$$
$$(Co\varepsilon dt)^{1/2}dW_3(t),$$

with,

$$\sigma_{11} = \left[\sigma_{11}-\sigma_{13}^2/\sigma_{33}\right]^{+1},$$
$$\sigma_{22} = \sigma_{22}^{+1},$$
$$\sigma_{13} = \left[\sigma_{13}-\sigma_{11}\sigma_{33}/\sigma_{13}\right]^{+1},$$
$$\sigma_{33} = \left[\sigma_{33}-\sigma_{13}^2/\sigma_{11}\right]^{+1},$$
$$\sigma_{11} = \sigma_u^2,$$
$$\sigma_{22} = \sigma_v^2,$$
$$\sigma_{33} = \sigma_w^2,$$
$$u = U + u_\sigma,$$
$$v = V + v_\sigma = v_\sigma,$$

and,

$$w = W + w_\sigma = w_\sigma.$$

The constant Co, is called the universal constant for the Lagrangian structure function. Note that the σ's refer to kinematic shear stresses, i.e., shear stress divided by density. A

variety of investigators have estimated a plethora of values for *Co* ranging from 1.6 to 10 and we have chosen a value of 5.7 (Rodean, 1996, page 8). ε is the mean rate of turbulence kinetic energy dissipation. $dW_1(t)$, $dW_2(t)$, and $dW_3(t)$ are uncorrelated, normally distributed variables with means of zero and standard deviations of 1.

Most random particle codes use an even simpler form of the equations as exemplified for the vertical component in the following expression:

$$dw = -\frac{Co\varepsilon}{2}\sigma_{33}w\,dt + \frac{1}{2}\left(1+\sigma_{33}w^2\right)\frac{\partial\sigma_{33}}{\partial z}\,dt + \left(Co\varepsilon\,dt\right)^{1/2}dW_3(t),$$

the first term on the right is called the memory term, the second term is the drift term and the third term is the random acceleration term.

In the surface stress layer, we have the following parameterizations:

$$u_* = k z\frac{\partial U}{\partial z},$$
$$\sigma_u = 2u_*,$$
$$\sigma_v = 2u_*,$$
$$\sigma_w = 1.3u_*,$$
$$\varepsilon = \frac{u_*^3}{k\left(z+z_0\right)},$$

and,

$$\sigma_{13} = \sigma_{uw} = u_*^2\left(1-\frac{z}{h}\right)^{3/2} - u_*^2,$$

with z_0 the roughness length and *k* the von Karman constant (chosen as 0.4) (Rodean, 1996, pages 59-64).

The initial values of u', v', and w' are given by:

$$u' = \sigma_u dW_1,$$
$$v' = \sigma_v dW_2,$$

and,

$$w' = \sigma_w dW_3.$$

Treatment of turbulence associated with walls and rooftops

The presence of walls and rooftops will produce gradients in the local wind that will induce turbulence. We deal with these effects by using a local coordinate system that has the u component aligned with the mean wind and a w normal to the mean wind in the direction with the largest increase in the wind speed. The required axes rotations are shown below.

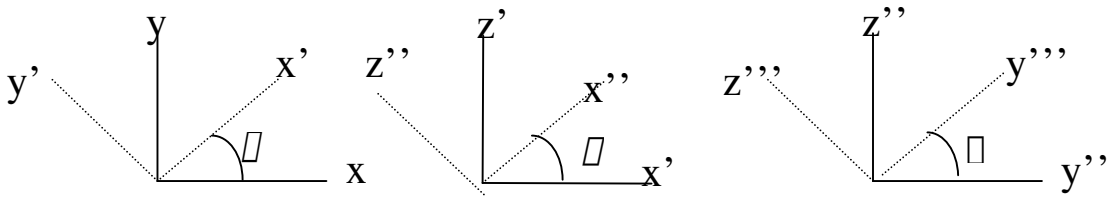

Fig. 1. The three rotations used in the wind-following coordinate system.

The first rotation produces the x' and y' axis through rotation through the angle α where

$$\alpha = \arctan\left(\frac{v}{u}\right).$$

The second rotation produces the x'' and z'' axes by rotation of the x' and z' axes through the angle β where

$$\beta = \arctan\left(\frac{w}{\sqrt{u^2 + v^2}}\right).$$

The third rotation produces the z''' and y''' axes from the z'' and y'' axes through rotation through the angle Γ. The angle Γ is calculated by optimizing the rate of change of the wind speed with respect to distance along the z''' axis,

$$\frac{\partial u'''}{\partial z'''} = \frac{\partial s}{\partial x}(\sin\alpha\sin\gamma - \cos\alpha\sin\beta\cos\gamma) - \frac{\partial s}{\partial y}(\cos\alpha\sin\gamma + \sin\alpha\sin\beta\cos\gamma) + \frac{\partial s}{\partial z}\cos\beta\cos\gamma,$$

with s the wind speed or u'''. The optimization results in the equation:

$$\gamma = \arctan\left(\frac{-\frac{\partial s}{\partial x}\sin\alpha + \frac{\partial s}{\partial y}\cos\alpha}{+\frac{\partial s}{\partial x}\cos\alpha\sin\beta + \frac{\partial s}{\partial y}\sin\alpha\sin\beta - \frac{\partial s}{\partial z}\cos\beta}\right)$$

which may result in a minimum rather than a maximum. If the above equation results in a minimum the appropriate value is found by replacing Π with $\Pi + \pi$.

Unit vectors in the triply-rotated system are described by:

$$i_{x'''} = \cos\phi\cos\psi i_x + \sin\phi\cos\psi i_y + \sin\psi i_z,$$
$$i_{y'''} = -(\cos\phi\sin\phi\sin\theta + \sin\phi\cos\theta) i_x - (\sin\phi\sin\phi\sin\theta - \cos\phi\cos\theta) i_y - \cos\phi\sin\theta\, i_z,$$

and,

$$i_{z'''} = (\sin\phi\sin\theta - \cos\phi\sin\phi\cos\theta) i_x - (\cos\phi\sin\theta + \sin\phi\sin\phi\cos\theta) i_y + \cos\phi\cos\theta\, i_z.$$

We describe transformations from the rotated system to the unrotated system with the equations:

$$u = u'''\alpha_1 + v'''\alpha_2 + w'''\alpha_3,$$
$$v = u'''\beta_1 + v'''\beta_2 + w'''\beta_3,$$

and,

$$w = u'''\gamma_1 + v'''\gamma_2 + w'''\gamma_3,$$

where,

$$\alpha_1 = \cos\phi\cos\psi,$$
$$\alpha_2 = -\sin\phi\cos\theta - \cos\phi\sin\psi\sin\theta,$$
$$\alpha_3 = \sin\phi\sin\theta - \cos\phi\sin\psi\cos\theta,$$
$$\beta_1 = \sin\phi\cos\psi,$$
$$\beta_2 = \cos\phi\cos\theta - \sin\phi\sin\psi\sin\theta,$$
$$\beta_3 = -\cos\phi\sin\theta - \sin\phi\sin\psi\cos\theta,$$
$$\gamma_1 = \sin\psi,$$
$$\gamma_2 = \cos\psi\sin\theta,$$

and,

$$\gamma_3 = \cos\psi\cos\theta.$$

We describe the transformations from the unrotated system to the rotated system in a similar fashion:

$$u''' = u\alpha_{n1} + v\alpha_{n2} + w\alpha_{n3},$$
$$v''' = u\beta_{n1} + v\beta_{n2} + w\beta_{n3},$$

and,

$$w''' = u\gamma_{n1} + v\gamma_{n2} + w\gamma_{n3},$$

with,

$$\alpha_{n1} = \cos\phi\cos\psi,$$
$$\alpha_{n2} = \sin\phi\cos\psi,$$
$$\alpha_{n3} = \sin\psi,$$
$$\beta_{n1} = -\sin\phi\cos\theta - \cos\phi\sin\psi\sin\theta,$$
$$\beta_{n2} = \cos\phi\cos\theta - \sin\phi\sin\psi\sin\theta,$$
$$\beta_{n3} = \cos\psi\sin\theta,$$

$$\alpha_{n1} = \sin\phi \sin\theta - \cos\phi \sin\psi \cos\theta ,$$
$$\alpha_{n2} = -\cos\phi \cos\theta - \sin\phi \sin\psi \cos\theta ,$$

and,

$$\alpha_{n3} = \cos\psi \cos\theta .$$

The parameterizations apply to the rotated coordinate system, but we also need to be able to describe the turbulent winds in the unrotated coordinate system. The above relationships can be used to describe the Reynolds stresses in the unrotated system in terms of the stresses and mean winds in the rotated system:

$$\overline{u_f^2} = \overline{u'''^2_f}\alpha_1^2 + s^2\alpha_1^2 + 2\overline{u'''_f v'''_f}\alpha_1\alpha_2 + 2\overline{u'''_f w'''_f}\alpha_1\alpha_3 + \overline{v'''^2_f}\alpha_2^2 + 2\overline{v'''_f w'''_f}\alpha_2\alpha_3 + \overline{w'''^2_f}\alpha_3^2 - \bar{u}^2 ,$$

$$\overline{v_f^2} = \overline{u'''^2_f}\alpha_1^2 + s^2\alpha_1^2 + 2\overline{u'''_f v'''_f}\alpha_1\alpha_2 + 2\overline{u'''_f w'''_f}\alpha_1\alpha_3 + 2\overline{v'''_f w'''_f}\alpha_2\alpha_3 + \overline{v'''^2_f}\alpha_2^2 + \overline{w'''^2_f}\alpha_3^2 - \bar{v}^2 ,$$

$$\overline{w_f^2} = \overline{u'''^2_f}\alpha_1^2 + s^2\alpha_1^2 + 2\overline{u'''_f v'''_f}\alpha_1\alpha_2 + 2\overline{u'''_f w'''_f}\alpha_1\alpha_3 + \overline{v'''^2_f}\alpha_2^2 + 2\overline{v'''_f w'''_f}\alpha_2\alpha_3 + \overline{w'''^2_f}\alpha_3^2 - \bar{w}^2 ,$$

$$\overline{u_f v_f} = \overline{u'''^2_f}\alpha_1\alpha_1 + s^2\alpha_1\alpha_1 + \overline{u'''_f v'''_f}(\alpha_1\alpha_2 + \alpha_2\alpha_1) + \overline{u'''_f w'''_f}(\alpha_1\alpha_3 + \alpha_3\alpha_1) + \overline{v'''^2_f}\alpha_2\alpha_2 + \overline{v'''_f w'''_f}(\alpha_2\alpha_3 + \alpha_3\alpha_2) + \overline{w'''^2_f}\alpha_3\alpha_3 - \bar{u}\bar{v} ,$$

$$\overline{u_f w_f} = \overline{u'''^2_f}\alpha_1\alpha_1 + s^2\alpha_1\alpha_1 + \overline{u'''_f v'''_f}(\alpha_1\alpha_2 + \alpha_2\alpha_1) + \overline{u'''_f w'''_f}(\alpha_1\alpha_3 + \alpha_3\alpha_1) + \overline{v'''^2_f}\alpha_2\alpha_2 + \overline{v'''_f w'''_f}(\alpha_2\alpha_3 + \alpha_3\alpha_2) + \overline{w'''^2_f}\alpha_3\alpha_3 - \bar{u}\bar{v} ,$$

and,

$$\overline{v_f w_f} = \overline{u'''^2_f}\alpha_1\alpha_1 + s^2\alpha_1\alpha_1 + \overline{u'''_f v'''_f}(\alpha_1\alpha_2 + \alpha_2\alpha_1) + \overline{u'''_f w'''_f}(\alpha_1\alpha_3 + \alpha_3\alpha_1) + \overline{v'''^2_f}\alpha_2\alpha_2 + \overline{v'''_f w'''_f}(\alpha_2\alpha_3 + \alpha_3\alpha_2) + \overline{w'''^2_f}\alpha_3\alpha_3 - \bar{v}\bar{w} ,$$

with the subscript f denoting a fluctuating or random component.

We use similar relationships to describe Reynolds stresses in the rotated system:

$$\overline{u'''^2_f} = \overline{u_f^2}\alpha_{n1}^2 + \bar{u}^2\alpha_{n1}^2 + 2\overline{u_f v_f}\alpha_{n1}\alpha_{n2} + 2\bar{u}\bar{v}\alpha_{n1}\alpha_{n2} + 2\overline{u_f w_f}\alpha_{n1}\alpha_{n3} + 2\bar{u}\bar{w}\alpha_{n1}\alpha_{n3} + \overline{v_f^2}\alpha_{n2}^2 + \bar{v}^2\alpha_{n2}^2 + 2\overline{v_f w_f}\alpha_{n2}\alpha_{n3} + 2\bar{v}\bar{w}\alpha_{n2}\alpha_{n3} + \overline{w_f^2}\alpha_{n3}^2 + \bar{w}^2\alpha_{n3}^2 - s^2 ,$$

$$\overline{v'''^2_f} = \overline{u_f^2}\alpha_{n1}^2 + \bar{u}^2\alpha_{n1}^2 + 2\overline{u_f v_f}\alpha_{n1}\alpha_{n2} + 2\bar{u}\bar{v}\alpha_{n1}\alpha_{n2} + 2\overline{u_f w_f}\alpha_{n1}\alpha_{n2} + 2\bar{u}\bar{w}\alpha_{n1}\alpha_{n3} + \overline{v_f^2}\alpha_{n2}^2 + \bar{v}^2\alpha_{n2}^2 + 2\overline{v_f w_f}\alpha_{n2}\alpha_{n3} + 2\bar{v}\bar{w}\alpha_{n2}\alpha_{n3} + \overline{w_f^2}\alpha_{n3}^2 + \bar{w}^2\alpha_{n3}^2 ,$$

$$\overline{w'''^2_f} = \overline{u_f^2}\alpha_{n1}^2 + \bar{u}^2\alpha_{n1}^2 + 2\overline{u_f v_f}\alpha_{n1}\alpha_{n2} + 2\bar{u}\bar{v}\alpha_{n1}\alpha_{n2} + 2\overline{u_f w_f}\alpha_{n1}\alpha_{n3} + 2\bar{u}\bar{w}\alpha_{n1}\alpha_{n3} + \overline{v_f^2}\alpha_{n2}^2 + \bar{v}^2\alpha_{n2}^2 + 2\overline{v_f w_f}\alpha_{n2}\alpha_{n3} + 2\bar{v}\bar{w}\alpha_{n2}\alpha_{n3} + \overline{w_f^2}\alpha_{n3}^2 + \bar{w}^2\alpha_{n3}^2 ,$$

and finally (the other shear stresses are not needed):

$$\overline{u'''_f w'''_f} = \overline{u_f^2}\,\delta_{n1}\delta_{n1} + \overline{u}^2\,\delta_{n1}\delta_{n1} + \overline{u_f v_f}(\delta_{n1}\delta_{n2} + \delta_{n2}\delta_{n1}) + \overline{u}\,\overline{v}(\delta_{n1}\delta_{n2} + \delta_{n2}\delta_{n1}) +$$
$$\overline{u_f w_f}(\delta_{n1}\delta_{n3} + \delta_{n3}\delta_{n1}) + \overline{u}\,\overline{w}(\delta_{n1}\delta_{n3} + \delta_{n3}\delta_{n1}) + \overline{v_f^2}\,\delta_{n2}\delta_{n2} + \overline{v}^2\,\delta_{n2}\delta_{n2} +$$
$$\overline{v_f w_f}(\delta_{n2}\delta_{n3} + \delta_{n3}\delta_{n2}) + \overline{v}\,\overline{w}(\delta_{n2}\delta_{n3} + \delta_{n3}\delta_{n2}) + \overline{w_f^2}\,\delta_{n3}\delta_{n3} + \overline{w}^2\,\delta_{n3}\delta_{n3}.$$

The equation for the dissipation remains:

$$\varepsilon = \frac{u_*^3}{k\left(d_{wall} + z_0\right)},$$

except that d_{wall} replaces z where d_{wall} is the smaller of z_{eff} and d_{wall}.

The analogy between the treatment of ground based shear and horizontal shear is flawed. In the case of a material surface the eddy-size is limited by the presence of the surface and u_* is calculated for the grid-cell nearest the surface. In the horizontal shear case there may or may not be a material surface and u_* is calculated cell by cell. In the first version of the model, the value of u_* associated with vertical wind-shear was based on the wind-shear at the ground or the rooftop and the same value was used for all heights above the ground or the roof.

Interpolation of winds to particle positions

We estimate the wind at position *(x,y,z)* by using an inverse distance interpolation among the neighboring grid-cell center values. We have:

$$i = \frac{x}{dx} + 1,$$

$$j = \frac{y}{dy} + 1,$$

and,

$$k = \frac{z}{dz} + 1,$$

so that, the expression for the interpolated *u*-component of the wind is:

$$u_{x,y,z} = \frac{\sum_{ii=i+1}^{i+1} \sum_{jj=j+1}^{j+1} \sum_{kk=k+1}^{k+1} \frac{u(ii,jj,kk)}{\sqrt{\left[\left(x_{ii} - x\right)^2 + \left(y_{jj} - y\right)^2 + \left(z_{kk} - z\right)^2\right]}}}{\sum_{ii=i+1}^{i+1} \sum_{jj=j+1}^{j+1} \sum_{kk=k+1}^{k+1} \frac{1}{\sqrt{\left[\left(x_{ii} - x\right)^2 + \left(y_{jj} - y\right)^2 + \left(z_{kk} - z\right)^2\right]}}},$$

with similar expressions for *v* and *w* components. The above expression applies when there are no walls between the point *(x,y,z)* and any of the adjacent grid-cell centers. If there is a wall, for example, in the plus *x* direction, the distance used in the inverse weight would be:

$$d_{x+} = i - dx - x,$$

instead of:

$$d_{i+1,j,k} - x,y,z = \sqrt{\left[\left(x_{i+1} - x\right)^2 + \left(y_j - y\right)^2 + \left(z_k - z\right)^2\right]},$$

with:

$$x_{ii} = \left(ii - 1\right) \bullet dx + .5 \bullet dx,$$

$$y_{jj} = \left(jj - 1\right) \bullet dy + .5 \bullet dy,$$

and:

$$z_{kk} = (kk - 1) \bullet dz + .5 \bullet dz.$$

The wind at the wall is identically zero and we are using the perpendicular distance to the wall that lies halfway between grid cell centers, while we use the distance to grid cell centers for points without intervening walls.

Treatment of reflection by walls

The approach to reflection is analogous to billiard ball type reflections. We estimate that reflection is required when we find that *icellflag(ii,jj,kk)* is one, where the grid indices *ii, jj,* and *kk* refer to the position (*xx,yy,zz)* after updating. The preceding position is (*x,y,z)* with associated indices *i,j,* and *k*; we know that *icellflag(i,j,k)* is zero, since the particle must begin in the atmosphere. If the change of only one index to its former value is sufficient to make *icellflag(i,jj,kk)* zero, we have wall reflection. For example if *icellflag(i,jj,kk)* is zero, we need to reflect the particle parallel to the x-axis. First, we define:

$$i_{sign} = \frac{(ii - i)}{\sqrt{(ii - i)^2}},$$

and,

$$i_{\max} = Max(ii, i),$$

and then estimate the distance from the new position within to wall to the surface of the wall as:

$$d_{xwall} = i_{sign}\left[x - (i_{\max} - 1)dx\right].$$

The new particle position after reflection is then:

$$x_{ref} = x - 2i_{sign}d_{xwall}.$$

We also reverse u, so that:

$$u_{ref} = -i_{sign}\sqrt{u^2}.$$

Similar equations apply to the case where the reflection is from a wall perpendicular to the y-axis or from a floor. However, we can also have the case where there is a corner reflection so that both the i and j indices must change in the time step for the particle to reach a wall or perhaps all three indices must change in the case of a particle approaching the corner of a roof from above. In each case, we estimate the penetration into the wall in the various directions and reflect about the direction for which the penetration is greatest. In this instance we define:

$$i_{sign} = \frac{(ii - i)}{\sqrt{(ii - i)^2}},$$

$$i_{\max} = Max(ii, i),$$

$$j_{sign} = \frac{(jj - j)}{\sqrt{(jj - j)^2}},$$

$$j_{\max} = Max(jj, j),$$

$$k_{sign} = \frac{(kk - k)}{\sqrt{(kk - k)^2}},$$

and,

$$k_{\max} = Max(kk, k).$$

The penetration into the wall in each direction is then:

$$d_{xwall} = i_{sign}\left[x - (i_{\max} - 1)dx\right],$$
$$d_{ywall} = j_{sign}\left[y - (j_{\max} - 1)dy\right],$$

and,

$$d_{zwall} = k_{sign}\left[z - (k_{\max} - 1)dz\right].$$

Once the direction of the greatest penetration is known, the reflection in that direction is estimated in a fashion similar to that described above for a wall reflection in the x-direction.

Concentration estimation

Average concentrations are estimated by:

$$\chi_{i,j,k} = \sum \frac{Q\Delta t_c}{n_{tot} dx_b dy_b dz_b t_{ave}},$$

where the sum is over all particles that are found within the sampling box *i,j,k* during the sampling time t_{ave}. n_{tot} is the total number of particles released during the computations, dx_b is the sampling box size in the x – direction, dy_b is the sampling box size in the y – direction, dz_b is the sampling box size in the z – direction, and Δt_c is the time between particle collection for concentration estimation.

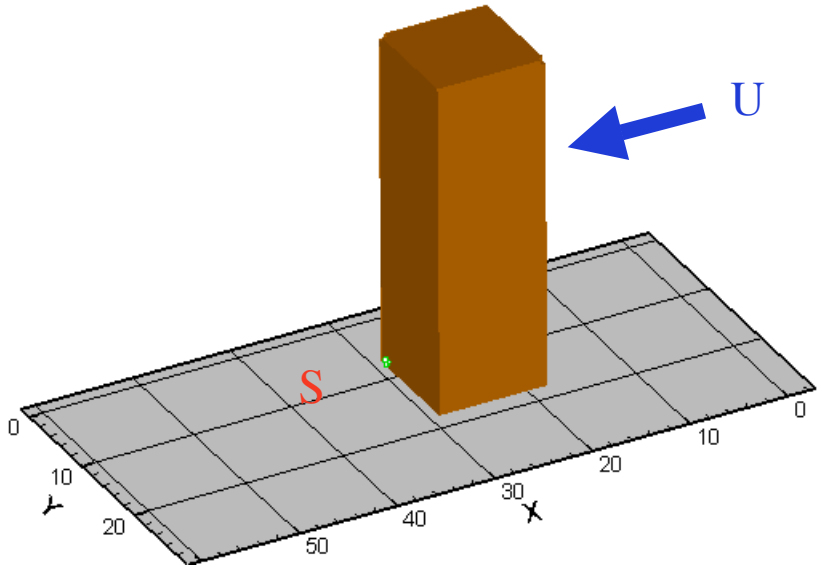

Figure2. Geometry of the high-rise wind tunnel experiment simulation. The source location is downwind of the 36 meter high building that has a base of 12 meters by 12 meters.

Model Test Case

We chose to simulate a wind-tunnel experiment carried out by EPA investigators (Ohba, Synder, and Lawson, 1993). The geometry of the release is shown in figure 1.

The study examined the concentrations associated with releases around one or two modeled high-rise buildings. We have made comparisons with the single building case and we have looked at a release a short distance from the backside of the building not far from the base of the building. Measurements of normalized concentrations,

$$\square_n = Uh^2 \square / Q$$

were available for the backside of the building and for a plane passing through the building centerline and parallel to the x-axis. The simulated building had a base of 12 by 12 meters and was 36 meters tall. We used winds of 3.5 m/s in our simulations. We modeled a release at 3 meters above ground and 6 meters behind the back wall. The release was simulated as particles released randomly from the surface of a sphere of radius .30 meters. This is a particularly challenging geometry, because of the rapid variations in the mean wind that are found in the wake of the building. In addition, the wall-effects play a major role because the release begins near the wall and drifts toward it. This simulation was compared to measured concentrations on the back wall of the highrise and to measured concentrations along the axis.

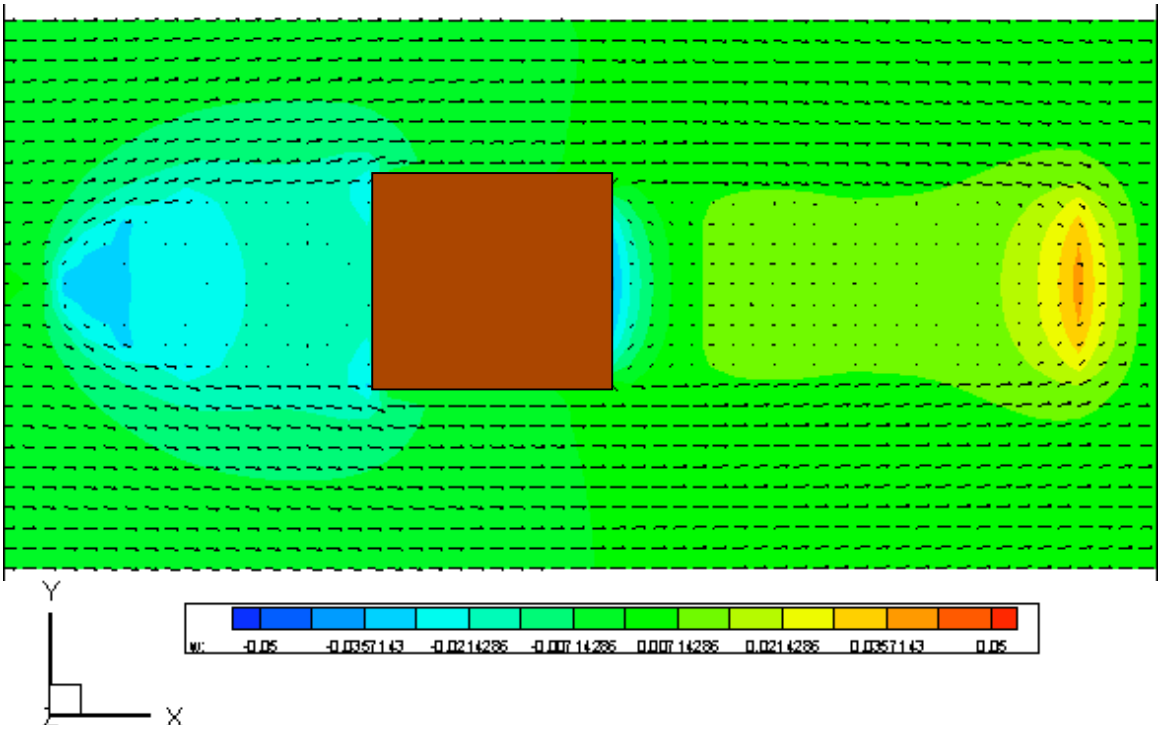

Figure 3. Wind vectors at 3 meters above the ground for the high-rise simulation.

Model Evolution

The initial version of the code exhibited several deficiencies when the test case was run. First, the code showed trapped particles so that it took a 16-minute simulation to produce a stable set of 2 minute-averaged concentrations for comparison with the measurements. In addition to the trapped particles, the model exhibited very compact concentration fields so that the concentration gradients were much greater than those found in the measured fields. One of the first efforts to improve the code focused on the dissipation

$$\varepsilon = \frac{u_*^3}{k\left(d_{wall} + z_0\right)},$$

where d_{wall} was modified to be the shortest distance to a wall rather than the distance to a wall in the crosswind direction. This change did not produce major changes in the concentration fields. The turbulence was also very low in the region of the release because the wind speeds were low.

The next improvement in the code focused on the use of local gradients everywhere so that friction velocity u_* is estimated by:

$$u_* = l_z \left| \frac{\partial u}{\partial z} \right|,$$

with l_z the height above ground multiplied by the von Karman constant k. Where there are flow reversals, we use

$$l_z = k \left| \frac{u}{\frac{\partial u}{\partial z}} \right|,$$

if it provides the smaller of the two expressions. The normal stresses are:

$$\sigma_{11} = \sigma_u^2 = \sigma_{22} = \sigma_v^2 = 4u_*^2; \qquad \sigma_{33} = 1.69u_*^2,$$

while the kinematic Reynolds shear stress, σ_{13}, and the dissipation, ε, are:

$$\sigma_{13} = l_z \frac{\partial u}{\partial z}, \qquad \varepsilon = \frac{u_*^3}{l_z}.$$

An additional term $u \frac{\partial u}{\partial x} dt$ was added to du to account for gradients along the mean wind. In addition the formulation of gradients was improved by the use of centered differences as opposed to backward differences. Also a limiting expression for derivatives of sigmas near a wall was developed, so that for approaching a vertical wall we would have:

$$\sigma_y \to ky \frac{1.3}{ky} l_y \left| \frac{\partial u}{\partial z} \right| + \left| \frac{\partial u}{\partial y} \right| \to ky \left| \frac{\partial u}{\partial y} \right|$$

since u is zero at the wall, and consequently

$$\frac{\partial \sigma_y}{\partial y} \to 1.3k \frac{u}{y},$$

which approaches a constant near the wall. Furthermore, we set a minimum u_* of 0.03 meters per second. We also modified the way in which the integration of the accelerations is carried out over the time step. The turbulent winds are referenced to the local coordinate system rather than the fixed coordinate system. The earlier form of the code used the random velocity at the start of the current time step as the value at the end of the last time step. However, as the winds are changing rapidly with distance the local coordinate system is changing orientation also. Consequently, the random component from the previous time step is referenced to a different coordinate system than that of the current time step. The current model converts random velocities to the fixed coordinate

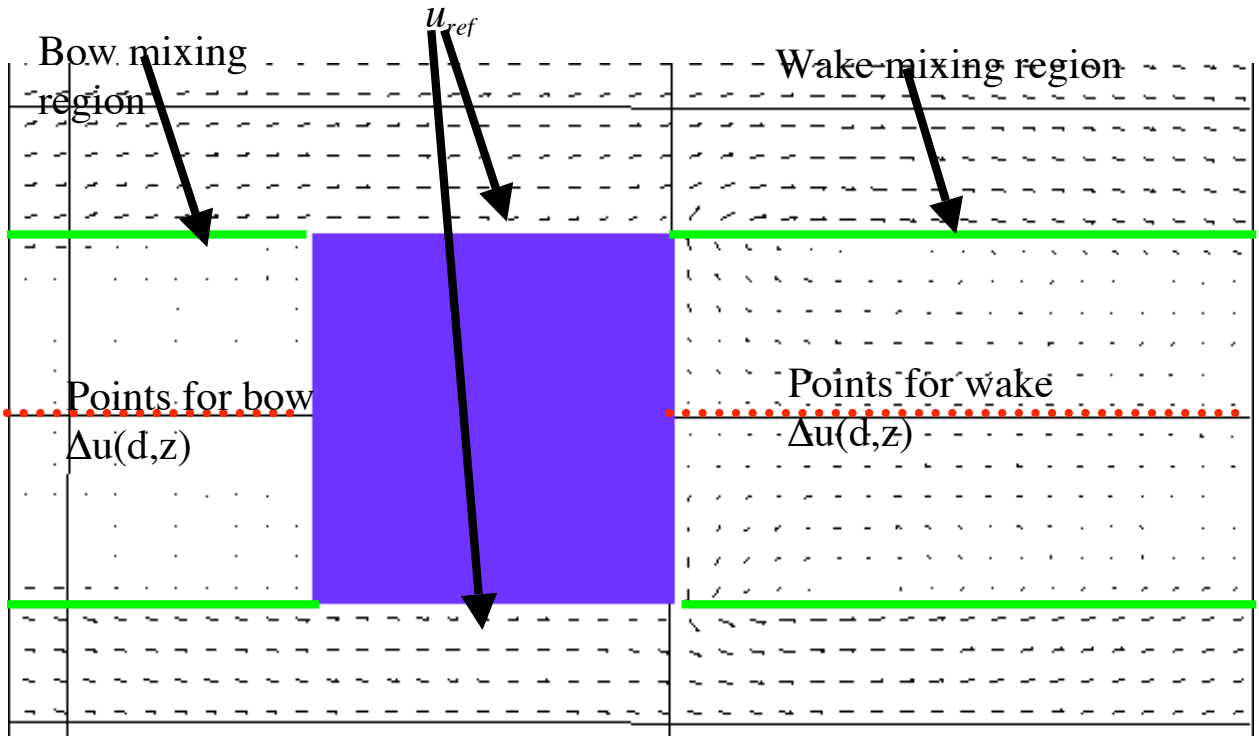

Fig. 4. Geometry for the deduction of u_{*g} for horizontal, non-local mixing.

system and then rotates them into the current local coordinate system before the integration is performed.

Treatment of Non-Local Mixing

Large-eddy simulations of flows around buildings exhibit eddies that sweep contaminants across the cavities and wakes of buildings. The measured concentrations suggest that there is considerable mixing in the wakes of buildings. This process was conceptualized as driven by velocity differences between the winds passing by the sides of buildings and the light winds along the axis of the wake or eddy. Two situations were considered, mixing produced by vertical axis eddies that mixed materials horizontally, and mixing produced by eddies that brought material down from the higher winds above the cavity or wake. In the case of horizontal mixing, the length scale, l_g, was chosen as the half-width of the wake or cavity and the velocity difference was calculated by comparing the winds at the edge of the building with those along the centerline of the wake or cavity:

$$\Delta u_{ref}(d,z) = s_{w/2+}(\frac{l}{2},z) - s_a(d,z)$$

where $s_{w/2+}$ is the wind speed just outside the building at its center in the lengthwise direction and $s_a(d,z)$ is the speed on the axis of the wake or cavity at a distance d from the nearest wall of the building. Non-local mixing is assumed to produce a non-local friction velocity of:

$$u_{*g} = k\,u_{ref}(d,z),$$

for all points inside the wake or cavity that satisfy:

$$s(d,y,z) < .8 * u_{ref}(d,z),$$

with y measured transverse to the downwind axis of the building. The effective width of the building and the length of the wake or eddy provide the region for which non-local mixing is considered. The parameters describing the wake or eddy are provided by QUIC-URB output as:

$$d_w = 3l_r$$

with d_w the distance from the back wall of the building to the end of the wake, and L_{fx} the distance in the x-direction to the upstream limit of the front eddy, and L_{fy} the distance in the y-direction to the upstream limit of the cavity. Figure 4 illustrates the geometry The coordinate system relevant to horizontal mixing is assumed to be aligned with the mean wind. In the coordinate system aligned with the mean wind we use:

$$\overline{u_{gf}^2} = 4u_{*g}^2,$$
$$\overline{w_{gf}^2} = 4u_{*g}^2,$$

and

$$\overline{v_{gf}^2} = 1.69u_{*g}^2.$$

For the shear stresses we use:

$$\overline{u_{gf}v_{gf}} = -\frac{y - y_a}{y_{w/2+}}u_{*g}^2$$

and

$$\overline{u_{gf}w_{gf}} = \overline{v_{gf}w_{gf}} = 0.$$

For mixing in the vertical direction (eddies whose axis is horizontal), the reference wind speed is that directly above the point of interest and it is compared to a zero speed at the ground or rooftop. We describe the friction velocity as:

$$u_{*gz}(d,y) = s_{ht+}(d,y)$$

with $s_{ht+}(d,y)$, the mean speed at the height of the building top plus one cell at a distance d from the building wall and a transverse distance y. The relevant stresses are:

$$\overline{u_{gf}^2} = 4u_{*gz}^2,$$
$$\overline{v_{gf}^2} = 4u_{*gz}^2,$$
$$\overline{w_{gf}^2} = 1.69u_{*gz}^2,$$
$$\overline{u_{gf}w_{gf}} = -u_{*gz}^2,$$

and,

$$\overline{u_{gf}v_{gf}} = \overline{v_{gf}w_{gf}} = 0.$$

The choice between horizontal mixing and vertical mixing is made based on the largest average gradient of the mean wind. Specifically if:

$$\frac{-u_{ref}(d,z)}{w_{teff}/2} \geq \frac{s(d,y,z)}{ht_{eff}},$$

the mixing is dominated by the horizontal mixing. Otherwise, vertical mixing is assumed. The same point in the wake or eddy may be influenced by more than one building and we choose the building that has the largest u_{*g}.

The stresses obtained by this approach are appropriate to the mean wind, so that we have to transform the values into the original coordinate system. The relevant relationships are:

$$\theta = \arctan\left(\frac{v_{ls}}{u_{ls}}\right),$$
$$u = u_g\cos(\theta) + v_g\sin(\theta),$$
$$v = -u_g\sin(\theta) + v_g\cos(\theta),$$
$$\overline{u_f^2} = \overline{u_{gf}^2}\cos^2(\theta) + \bar{u}^2\cos^2(\theta) - 2\overline{u_{gf}v_{gf}}\cos(\theta)\sin(\theta) - 2\bar{u}\bar{v}\cos(\theta)\sin(\theta) + \overline{v_{gf}^2}\sin^2(\theta) + \bar{v}^2\sin^2(\theta) - \bar{u}^2,$$
$$\overline{v_f^2} = \overline{u_{gf}^2}\sin^2(\theta) + \bar{u}^2\sin^2(\theta) + 2\overline{u_{gf}v_{gf}}\cos(\theta)\sin(\theta) + 2\bar{u}\bar{v}\cos(\theta)\sin(\theta) + \overline{v_{gf}^2}\cos^2(\theta) + \bar{v}^2\cos^2(\theta) - \bar{v}^2$$
$$\overline{u_f v_f} = \overline{u_{gf}^2}\cos(\theta)\sin(\theta) + \bar{u}^2\cos(\theta)\sin(\theta) + \overline{u_{gf}v_{gf}}\left(\cos^2(\theta) - \sin^2(\theta)\right) + \bar{u}\bar{v}\left(\cos^2(\theta) - \sin^2(\theta)\right) - \overline{v_{gf}^2}\sin(\theta)\cos(\theta) - \bar{v}^2\sin(\theta)\cos(\theta) - \bar{u}\bar{v},$$
$$\overline{u_f w_f} = \overline{u_{gf}w_{gf}}\cos(\theta) + \bar{u}\bar{w}\cos(\theta) - \overline{v_{gf}w_{gf}}\sin(\theta) - \bar{u}\bar{w}\sin(\theta) - \overline{uw},$$

and,

$$\overline{v_f w_f} = \overline{u_{gf}v_{gf}}\sin(\theta) + \bar{u}\bar{w}\sin(\theta) + \overline{v_{gf}w_{gf}}\cos(\theta) + \bar{v}\bar{w}\cos(\theta) - \bar{v}\bar{w}.$$

With v_{ls}, the large scale v-component of the mean wind and u_{ls} the large scale u-component of the mean wind.

Model Performance

The addition of the non-local mixing made a major improvement in the code. The concentration fields are much better matched to the measured concentrations, as shown in Figure 5. The source location is in red while the black dots show the sampling grid.

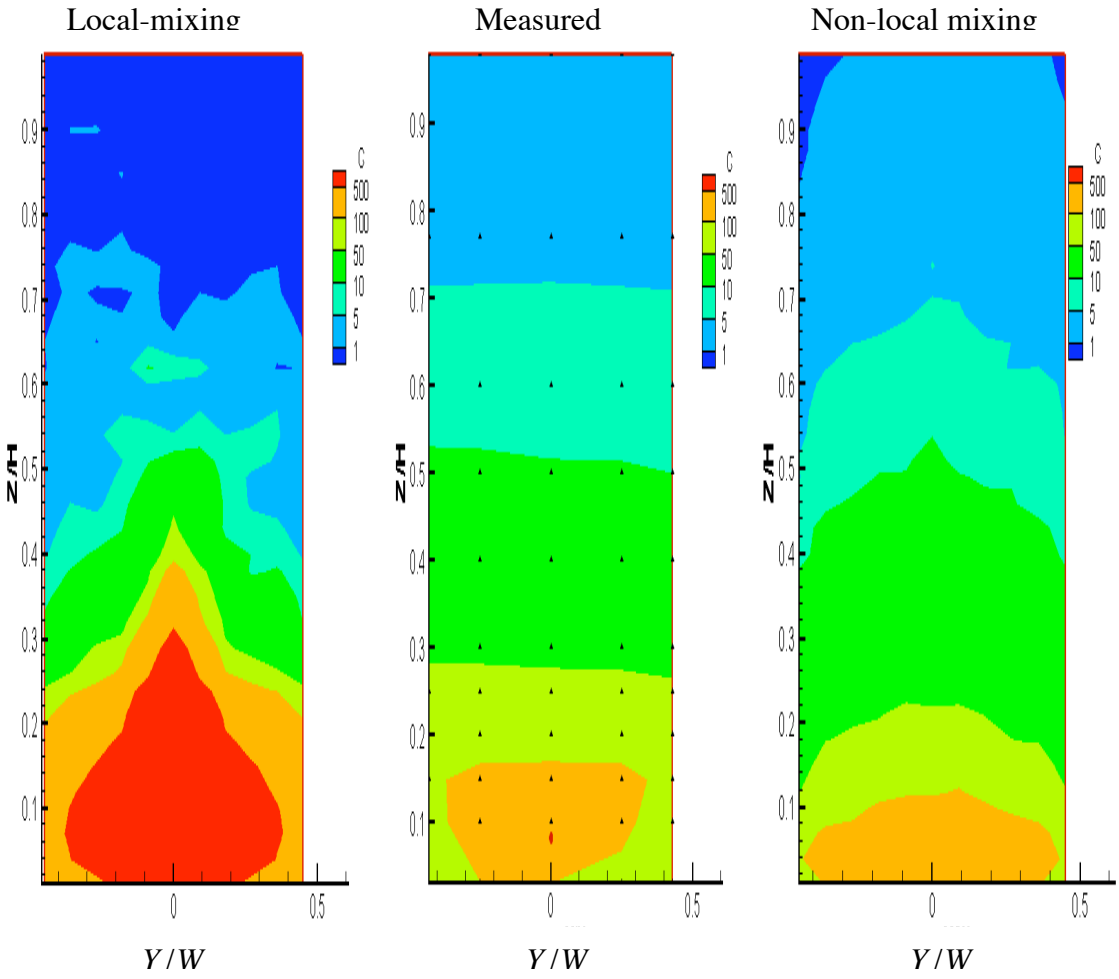

Figure 5. Comparison between measured (center) and simulated (left –local mixing and right non-local mixing) along the back wall of the highrise building. The source location is indicated by the red dot, while the black dots report the locations of the measurements.

The pattern of the simulated, local-mixing concentrations is much different than the measurements, while the non-local mixing simulation gives much better agreement. The highest measured concentrations at the back wall are 116 normalized, while the normalized concentration for the local-gradient simulation is 6144. The non-local simulation produces a normalized, back wall maximum concentration of 177.

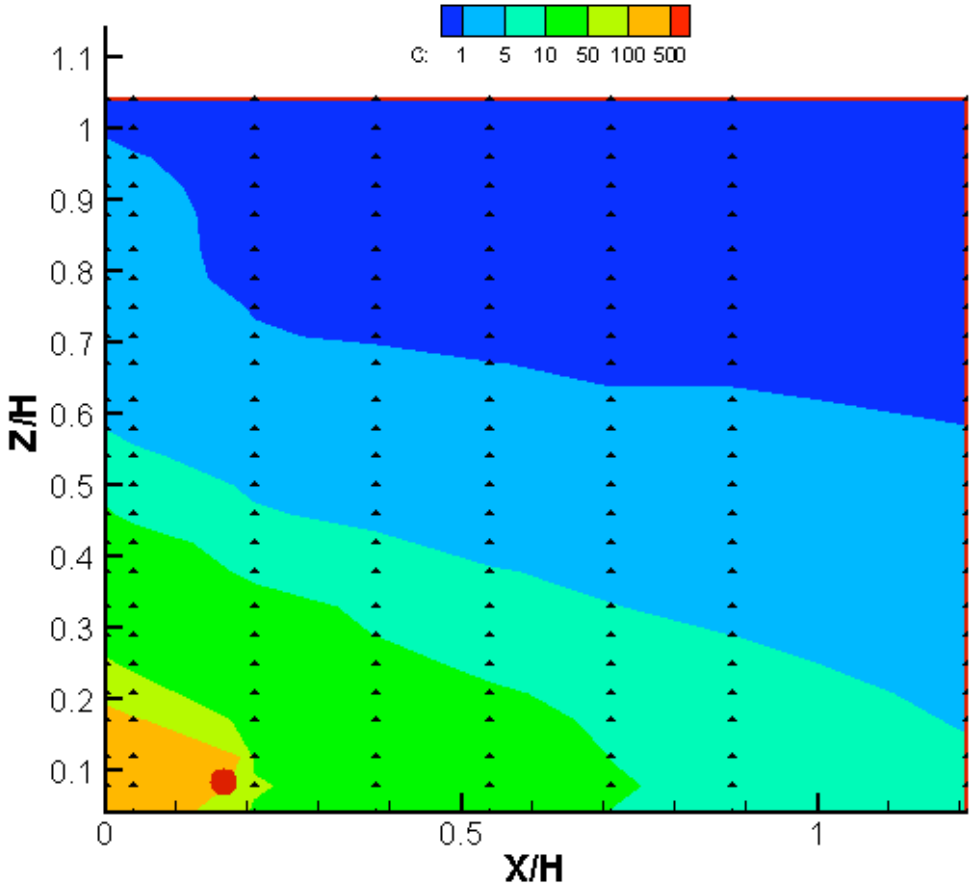

Figure 6. Measured, normalized concentrations along the centerline of the building displayed as a function of the down wind distance divided by the building height. The source location is shown by the red dot, while black triangles show the measurement locations.

The down-axis measurements and simulations show a similar behavior. Figure 6 shows the measured concentrations while Figure 7 displays the concentrations estimated with a non-local mixing model. The estimated concentrations are similar to those found in the measurements. Figure 8 depicts the estimated concentrations using the local-mixing version of the model. Once again the local-mixing version produces much different concentrations. The highest measured, normalized concentration is 508, while the non-local mixing model produces 726 at a point near the source position. The local mixing model produces a high of 6771 with concentrations as high as 6172 at the back wall of the building

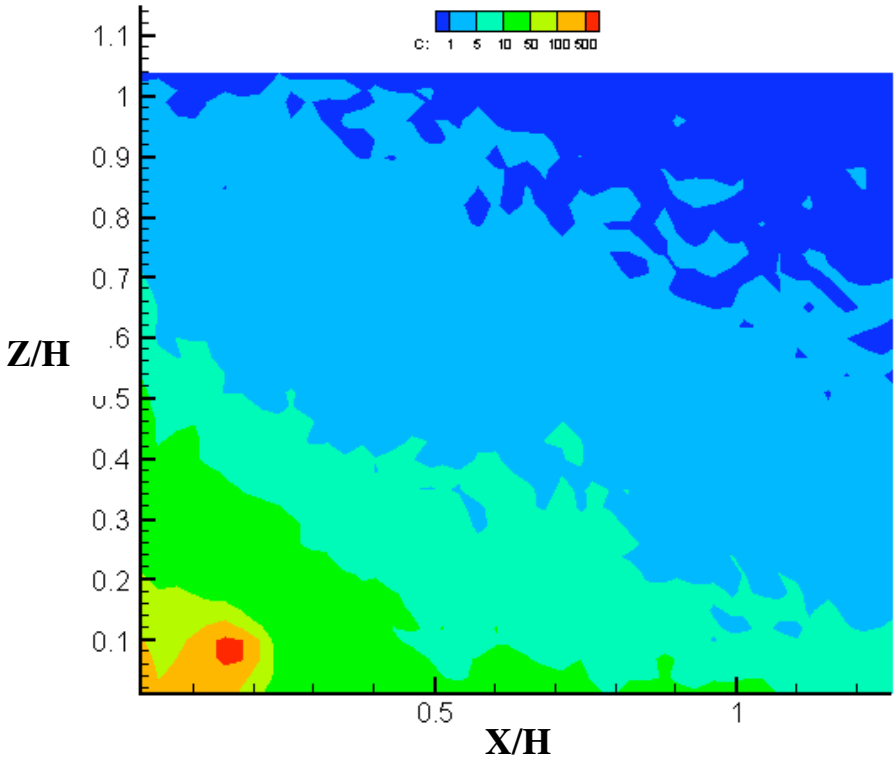

Figure 7. Estimated concentrations downwind of the building along the building centerline produced by the non-local mixing version of the model.

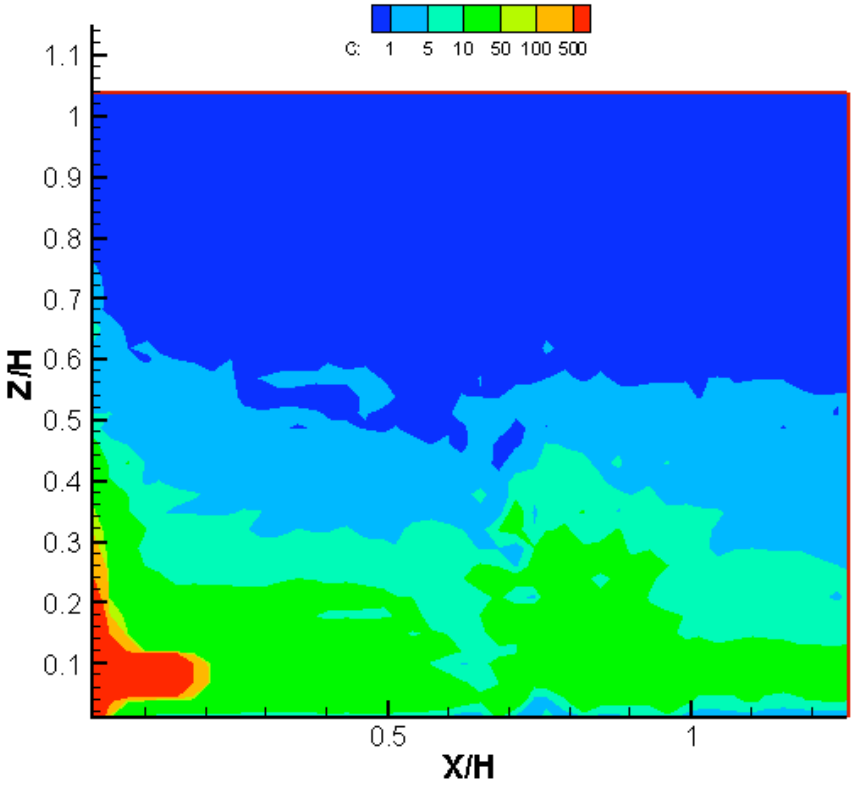

Figure 8. Estimated down-axis concentrations produced by a local-mixing version of the model.

References

Pardyjak, Eric R. and Michael J. Brown, 2001, Evaluation of a Fast-Response Urban Wind Model – Comparison to Single-Building Wind Tunnel Data, LA-UR-01-4028, Los Alamos National Laboratory.

Rodean, Howard C., 1996, "*Stochastic Lagrangian Models of Turbulent Diffusion,"* The American Meteorological Society, 82 pages.